Available online at www.sciencedirect.com
ScienceDirect
International Journal of Heat and Mass Transfer 50 (2007) 5215–5225
International Journal of HEAT and MASS TRANSFER
www.elsevier.com/locate/ijhmt

Correlation for boiling heat transfer of R-134a in horizontal tubes including effect of tube diameter

Shizuo Saitoh [a,*], Hirofumi Daiguji [b], Eiji Hihara [b]

[a] Department of Mechanical Engineering, The University of Tokyo, 7-3-1 Hongo, Bunkyo-ku, Tokyo 113-8656, Japan
[b] Institute of Environmental Studies, Graduate School of Frontier Sciences, The University of Tokyo, 7-3-1 Hongo, Bunkyo-ku, Tokyo 113-8656, Japan

Received 19 January 2006
Available online 10 August 2007

Abstract

A Chen-type correlation for flow boiling heat transfer of R-134a in horizontal tubes was modified taking into account the effect of tube diameter. The effect of tube diameter on flow boiling heat transfer coefficient was characterized by the Weber number in gas phase. Results showed that this correlation could be applied to a wide range of tube diameters (0.5–11-mm-ID). In addition, the dryout point and the heat transfer characteristics after the dryout point were also investigated based on the annular flow model. The proposed experimental expressions to predict both the dryout quality and the post-dryout heat transfer coefficient could also be applied to a wide range of tube diameter (0.5–11-mm-ID).

1. Introduction

High efficiency, compact heat exchangers have recently attracted much attention in their use in air conditioning systems due to possible energy conservation. Fundamental data on boiling heat transfer such as heat transfer coefficient and pressure drop is essential for design and operation of heat exchangers. Despite extensive experimental data on flow boiling heat transfer in small-diameter tubes (<3-mm-ID), the general characteristics such as the heat transfer mechanism in flow boiling and in pressure drop have not yet been clarified. In our previous study [1], the effect of tube diameter on the boiling heat transfer of refrigerant R-134a was experimentally investigated in horizontal small-diameter tubes (0.51-, 1.12-, and 3.1-mm-ID). Results showed that as the tube diameter decreased: (i) contribution of forced convective evaporation to boiling heat transfer decreased; (ii) onset of dryout occurred in a lower quality region; (iii) prediction of the pressure drop by using a homogeneous model was better than that by using the Lockhart–Martinelli correlation; and (iv) local heat transfer coefficient decreased at high vapor quality, when the flow pattern changed from continuous flow (annular flow) to intermittent flow (slug or plug flow) at the inlet of the tube. In 6-mm-ID tubes, the onset of dryout occurred at vapor quality $x = 0.9$, whereas in 0.51-mm-ID tubes, it occurred at $x = 0.6$. Therefore, prediction of both the onset of dryout and the post-dryout heat transfer coefficient is crucial in the design of compact heat exchangers.

The flow boiling heat transfer in a tube is generally expressed as the sum of two mechanisms, namely, nucleate boiling and film evaporation, and most correlations for boiling heat transfer coefficient consist of a nucleate boiling term and a forced convective term [2]. Numerous correlations to predict the flow boiling heat transfer coefficient have been proposed for different working fluids and various experimental conditions [3–6]. The Chen-type correlation is a well-known correlation for saturated flow boiling, in which flow boiling heat transfer is represented as the summation of a micro-convective (nucleate boiling) contribution and a macro-convective (forced convective evaporation) contribution [7]. Chen introduced two factors: F, which is an enhancement factor for the contribution from forced convection and is represented as a

* Corresponding author. Tel./fax: +81 3 5841 6325.
E-mail address: saitoh@hee.k.u-tokyo.ac.jp (S. Saitoh).

0017-9310/$ - see front matter © 2007 Elsevier Ltd. All rights reserved.
doi:10.1016/j.ijheatmasstransfer.2007.06.019

Nomenclature

A	cross-sectional area of a tube, m^2
A_D	ratio of dry-portion around the tube perimeter
A_v	cross-sectional area of the vapor core, m^2
Bo	boiling number
C_g	friction factor for gas, $C_g = 0.046$
C_l	friction factor for liquid, $C_l = 16$
Co	convection number used in the Kandlikar correlation
c_{pl}	specific heat at constant pressure in the liquid phase, J/kg K
D	inside diameter of a tube, m
F	enhancement factor used by Chen [7]
F_K	fluid-dependent parameter used in the Kandlikar correlation
Fr	Froude number
G	mass flux, kg/m^2 s
g	acceleration of gravity, m/s^2
H_{lg}	latent heat of evaporation, J/kg
h	heat transfer coefficient, W/m^2 K
h_{exp}	experimental boiling heat transfer coefficient, W/m^2 K
h_l	liquid-phase heat transfer coefficient, W/m^2 K; $Re_l > 1000$, $h_l = 0.023\frac{\lambda_l}{D}\left(\frac{G_l D}{\mu_l}\right)^{0.8}\left(\frac{c_{pl}\mu_l}{\lambda_l}\right)^{1/3}$; $Re_l < 1000$, $h_l = \frac{4.36\lambda_l}{D}$
h_{TP}	two-phase boiling heat transfer coefficient, W/m^2 K
L	heated tube length, m
Pr	Prandtl number
p	pressure, Pa
q	heat flux, W/m^2
Re	Reynolds number $Re_l = \frac{G_l D}{\mu_l}, Re_g = \frac{G_g D}{\mu_g}$
S	suppression factor used by Chen
s	slip ratio u_g/u_l
T	temperature, K
u	fluid mean velocity in two-phase flow
We	Weber number
x	vapor quality
x_{dryout}	dryout vapor quality
X	Lockhart–Martinelli parameter; $Re_l > 1000$, $Re_g > 1000$: $X = \left(\frac{1-x}{x}\right)^{0.9}\left(\frac{\rho_g}{\rho_l}\right)^{0.5}\left(\frac{\mu_l}{\mu_g}\right)^{0.1}$; $Re_l < 1000$, $Re_g > 1000$: $X = \left(\frac{C_l}{C_g}\right)^{0.5} Re_g^{-0.4}\left(\frac{G_l}{G_g}\right)^{0.5}\left(\frac{\rho_g}{\rho_l}\right)^{0.5}\left(\frac{\mu_l}{\mu_g}\right)^{0.5}$

Greek symbols

β	void fraction
θ	angle, rad
λ	thermal conductivity, W/mK
δ	liquid film thickness, m
δ_{crit}	critical liquid film thickness, m
μ	viscosity, Pa s
ρ	density, kg/m^3
σ	surface tension, N/m

Subscripts

cal	calculated
crit	critical
dryout	dryout of liquid film
g	gas-phase, vapor-phase
l	liquid-phase
nor	normalized
pool	pool boiling
post	post-dryout
pre	pre-dryout
TP	two-phase

function of the Lockhart–Martinelli parameter, and S, which is a suppression factor for the contribution from nucleate boiling and is represented as a function of a two-phase Reynolds number. Gungor and Winterton [8] proposed a modified Chen correlation from a vast amount of data (over 4300 data points) for saturated boiling heat transfer and sub-cooled boiling heat transfer. Assuming that boiling heat transfer is improved by significant disturbance of a boundary layer adjacent to the heat transfer surface, they modified F as a function of boiling number Bo and Lockhart–Martinelli parameter X. They also proposed a simplified correlation in which contributions of both forced convection and nucleate boiling were expressed by the enhancement factor because experimental data show that the contribution from nucleate boiling is smaller than that from film evaporation [9]. Shah [10] proposed a correlation for the heat transfer coefficient as a function of three dimensionless parameters: convection number Co, Bo, and Froude number Fr. Kandlikar [11] proposed a correlation for the heat transfer coefficient in which the convective boiling term is expressed as a function of Co, the nucleate boiling term as a function of Bo, and a fluid-dependent parameter F_K. Although numerous correlations have been proposed to date, most cannot be applied beyond the range of their experimental conditions.

At the point where a liquid film in annular flow in a tube disappears, the temperature of the tube wall increases and the local heat transfer coefficient decreases sharply. This point is called the dryout point. Chaddock and Varma [12] experimentally investigated dryout with R-22 flowing in a 3/8-in.-OD horizontal tube and reported that dryout occurred at $0.89 < x < 0.99$ and that the dry-portion extended from the top of the tube to the bottom. Katto [13,14] reported the conditions for the critical heat flux

(CHF) in a uniformly heated vertical tube. He classified the CHF into two types depending on whether the relation between CHF and the sub-cooled enthalpy of fluid at the inlet of a tube is linear or non-linear, and classified it further into four regimes (L-, H-, N-, and HP-regimes) using a non-dimensional number $\left(\frac{G^2L}{\rho_l\sigma}\right)$. Dryout of the liquid film on a tube wall at high x corresponds to the L-regime CHF. Sun and Groll [15] proposed a model to predict the onset of dryout for carbon dioxide flow boiling in horizontal tubes, and reported that their model for carbon dioxide could be used for other refrigerants. Although the prediction of dryout point is crucial in the design of compact heat exchangers using small tubes, studies on this topic are limited.

In this current study, a correlation for flow boiling heat transfer of R-134a in horizontal tubes was developed to aid in the design of compact heat exchangers that utilize small tubes. First, a Chen-type correlation for flow boiling heat transfer was modified by considering the effect of tube diameter by using the Weber number to represent this effect. Then, to predict the dryout quality, a simple annular flow model was developed, and the post-dryout heat transfer characteristics were investigated.

2. Flow boiling heat transfer and dryout quality

2.1. Pre-dryout heat transfer

Although numerous correlations for flow boiling have been proposed, the boiling heat transfer mechanisms have not yet been clarified to date because the heat transfer of flow boiling is strongly related to complex flow patterns of two-phase flow. In this study, a modified Chen-type correlation was proposed by fitting flow boiling data over a wide range of tube diameters (0.5–11-mm-ID). In the original Chen correlation for saturated flow boiling [7], the heat transfer coefficient consists of a convective boiling contribution (Fh_l) and a nucleate boiling contribution (Sh_{pool}) as follows:

$$h_{TP,pre} = Fh_l + Sh_{pool}, \tag{1}$$

where h_l is the heat transfer coefficient based on the Dittus–Boelter's equation only for liquid flow in a tube and h_{pool} is the heat transfer coefficient based on the Forster and Zuber relation for nucleate pool boiling. The factor F related to the Martinelli parameter X represents the enhancement of forced convection heat transfer, and the factor S related to the two-phase Reynolds number Re_{TP} represents the suppression of boiling heat transfer due to decrease in superheat of the liquid film on a tube wall with increasing forced convection effect. In general, as x increases, vapor velocity increases and the contribution of convective evaporation increases, while the contribution of nucleate boiling decreases because the superheat of the liquid film decreases due to film evaporation.

As the tube diameter decreases, the surface tension rather than the buoyancy affects the two-phase flow. The predominance of surface tension over buoyancy leads to the insensitivity of channel orientation with respect to gravity, and reduces the difference in velocity between liquid and vapor phases (slip velocity) [16,17]. This reduction in slip velocity suppresses the generation of shear stress at the vapor–liquid interface and also suppresses the occurrence of interfacial waves. In this study, the effect of tube diameter D on the fluid flow conditions is expressed by using the Weber number, $We_g = G_g^2D/\sigma\rho_g$. Furthermore, because the fluid flow conditions more strongly affect forced convective evaporation than nucleate boiling, the factor F for forced convective heat transfer is expressed explicitly as a function of We_g. In summary, F is expressed as a function of X and We_g, $F = f(X, We_g)$, whereas S for suppression of nucleate boiling is expressed as a function of Re_{TP} defined as $Re_{TP} = Re_lF^{1.25}$:

$$F = 1 + \frac{\left(\frac{1}{X}\right)^l}{1 + We_g^m}, \tag{2}$$

$$S = \frac{1}{1 + a\left(Re_{TP} \times 10^{-4}\right)^n}. \tag{3}$$

The h_{pool} in Eq. (1) is calculated by the Stephan–Abdelsalam's correlation for organic refrigerants [18]:

$$h_{pool} = 207\frac{\lambda_l}{d_b}\left(\frac{qd_b}{\lambda_lT_l}\right)^{0.745}\left(\frac{\rho_g}{\rho_l}\right)^{0.581}Pr_l^{0.533}, \tag{4}$$

where d_b is the bubble departure diameter of nucleate boiling and given by

$$d_b = 0.51\left[\frac{2\sigma}{g(\rho_l - \rho_g)}\right]^{0.5}. \tag{5}$$

The parameters a, l, m, and n were determined by fitting 2224 data points from our previous study [1] and four other studies on saturated flow boiling inside horizontal tubes for refrigerant R-134a for $0.51 < D < 10.92$ mm [19–22], to our modified Chen-type correlation. The properties of refrigerant R-134a are calculated using REFPROP version 6.01 [23]. The resulting values in the fitting are $a = 0.4$, $l = 1.05$, $m = -0.4$ and $n = 1.4$. In Eq. (2), F decreases with decreasing We_g. At a constant mass flux, the surface force rather than the inertia force increases with decreasing D, resulting in suppression of the contribution of forced convective evaporation to the boiling heat transfer.

Figs. 1a–c compare the experimental h and calculated h based on our modified Chen-type correlation, the Kandlikar correlation [11], and the Gungor–Winterton correlation [9] for refrigerant R-134a in horizontal smooth tubes with $0.51 < D < 10.92$-mm-ID. Table 1 summarizes the Kandlikar and Gungor–Winterton correlations. When the superficial liquid Re, Re_l, is smaller than 1000, flow in the liquid phase is laminar and $h_l = 4.36\lambda_l/D$. In the Kandlikar correlation, the fluid-dependent parameter F_K

[24] of refrigerant R-134a was assumed to be 1.0. The h_{cal} based on our modified Chen-type correlation agreed well with h_{exp} for a wide range of D. However, h_{cal} that was calculated with the Kandlikar and Gungor–Winterton correlations did not agree well with h_{exp} for tubes with small D (0.51- and 1.12-mm ID). Table 2 lists the mean deviation and accuracy (defined as the fraction of data within ±30% error) for each of the three correlations. Our modified Chen-type correlation showed improved mean deviation and accuracy (13.6% and 93.6%, respectively) compared with either the Kandlikar correlation (19.7% and 80.7%) or Gungor and Winterton correlation (20.5% and 77.5%).

2.2. Dryout quality

In low heat flux conditions, such as in air conditioning systems and refrigerators, a liquid film disappears at high x due to evaporation of a liquid film on the inside wall of a tube. This disappearance is usually called *film dryout* or simply *dryout*, and the flow regime in the tube is generally

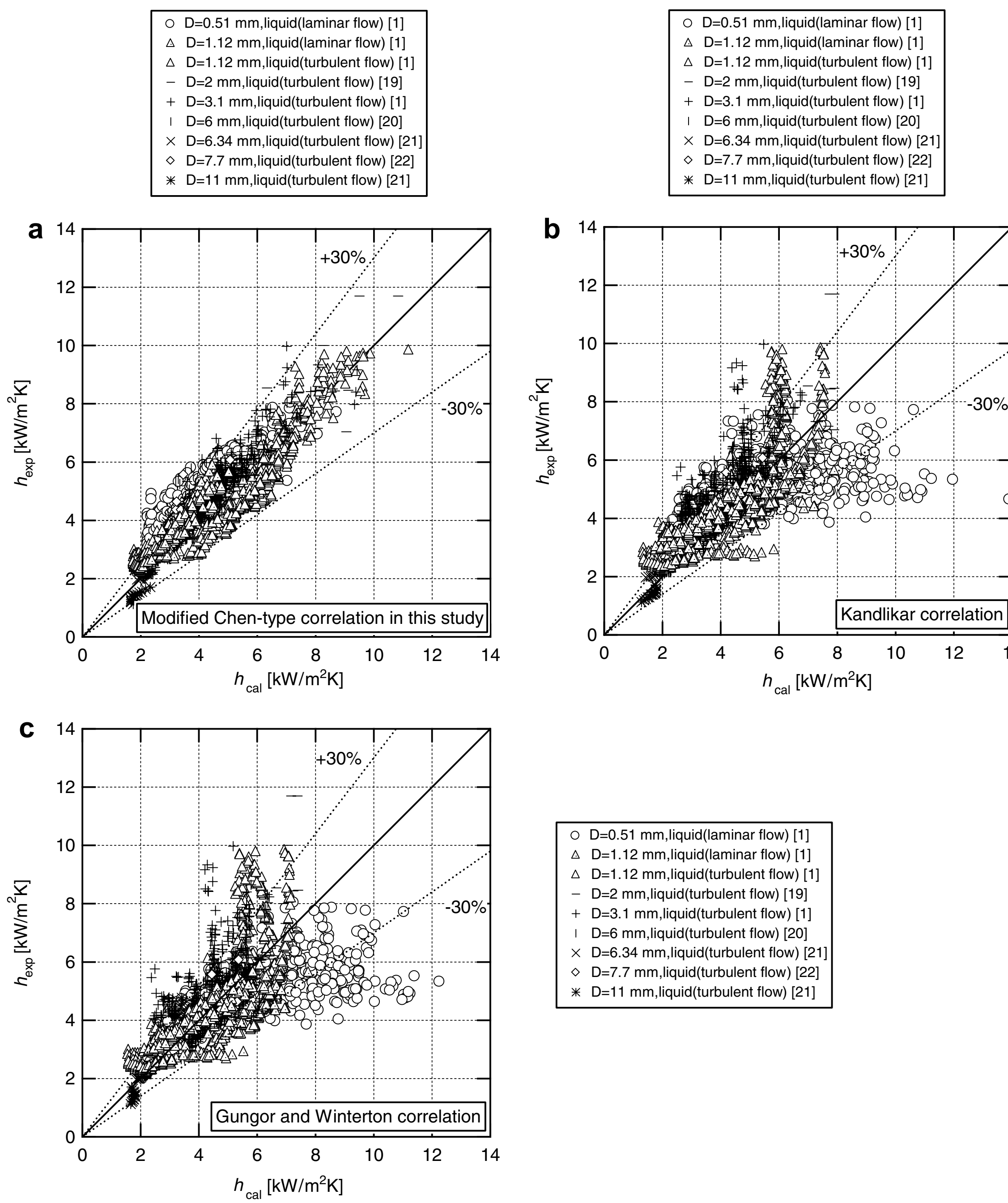

Fig. 1. Experimental flow boiling heat transfer coefficient h_{exp} vs. calculated h_{cal} for refrigerant R-134a in horizontal smooth tubes with 0.51–10.92-mm-ID based on (a) our modified Chen-type correlation, (b) Kandlikar correlation [11], and (c) Gungor and Winterton correlation [9].

annular flow. The occurrence of film dryout can be predicted by solving a mass balance equation for a liquid film in annular flow [25]. In this study, the x at which dryout occurs (x_{dryout}) in annular flow was predicted under the following three assumptions:

(1) The thickness of the liquid film is uniform.
(2) There is no entrainment or deposition of droplets between the vapor core and the liquid film.
(3) Heat transfer through the liquid film is conductive.

Fig. 2 illustrates the annular flow model in two-phase flow. If a local heat transfer coefficient h is known, then the liquid film thickness δ is given by

$$\delta = \frac{\lambda_l}{h}, \tag{6}$$

where λ_l is thermal conductivity of the liquid film. Void fraction β is defined as

$$\beta = \frac{A_v}{A} = \left(1 - \frac{2\delta}{D}\right)^2, \tag{7}$$

where A and A_v are the cross-sectional areas of the tube and vapor core, respectively. The void fraction β can also be expressed as

$$\beta = \frac{x}{x + s(1-x)\frac{\rho_g}{\rho_l}}, \tag{8}$$

where s is slip ratio, which is the ratio between the vapor mean velocity u_g and liquid mean velocity u_l. Assuming that the momentum and energy dissipation in the steady-state annular flow (see Fig. 2) are minimum, s can be expressed as [26]

$$s = \left(\frac{\rho_l}{\rho_g}\right)^{0.5} \quad \text{(minimum momentum)}, \tag{9}$$

$$s = \left(\frac{\rho_l}{\rho_g}\right)^{\frac{1}{3}} \quad \text{(minimum energy dissipation)}. \tag{10}$$

Based on Levy's momentum model [27], s is given by

$$s = \left(\frac{\beta\rho_l}{2\rho_g}\right)^{0.5}. \tag{11}$$

By eliminating β from Eqs. (7) and (8), the relation between x and δ is obtained. The dryout quality x_{dryout} can be expressed by using the critical liquid film thickness δ_{crit}, which is given by Eq. (6) using experimental data of h_{exp} just before the occurrence of dryout:

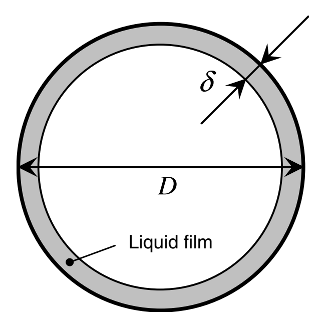

Fig. 2. Annular flow model. D is the inner diameter of a tube and δ is the liquid film thickness.

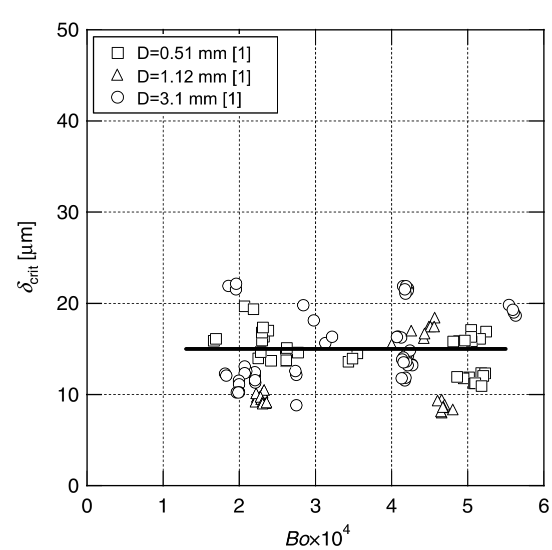

Fig. 3. Critical thickness of liquid film δ_{crit}vs. boiling number Bo. Line shows average δ_{crit}.

Table 1
Correlations for flow boiling heat transfer

	Correlation for flow boiling heat transfer
Gungor and Winterton [9]	$h_{TP} = Eh_l$ where $h_l = 0.023\frac{\lambda_l}{D}\left(\frac{G(1-x)D}{\mu_l}\right)^{0.8}\left(\frac{c_{pl}\mu_l}{\lambda_l}\right)^{0.4}$ $E = 1 + 3000Bo^{0.86} + 1.12\left(\frac{x}{1-x}\right)^{0.75}\left(\frac{\rho_l}{\rho_g}\right)^{0.41}$ If the tube is horizontal and the Froude number Fr_l is less than 0.05 then E should be multiplied by the factor $E_2 = Fr_l^{(0.1-2Fr_l)}$
Kandlikar [11]	$h_{TP} = h_l\left[C_1 Co^{C_2}(25Fr_{lo})^{C_5} + C_3 Bo^{C_4} F_K\right]$ where $h_l = 0.023\frac{\lambda_l}{D}\left(\frac{G(1-x)D}{\mu_l}\right)^{0.8}\left(\frac{c_{pl}\mu_l}{\lambda_l}\right)^{0.4}$ $Co = \left(\frac{1-x}{x}\right)^{0.8}\left(\frac{\rho_g}{\rho_l}\right)^{0.5}$ for $Co < 0.65$: $C_1 = 1.136$, $C_2 = -0.9$, $C_3 = 667.2$, $C_4 = 0.7$, $C_5 = 0.3$ $Co > 0.65$: $C_1 = 0.6683$, $C_2 = -0.2$, $C_3 = 1058$, $C_4 = 0.7$, $C_5 = 0.3$ $C_5 = 0$ for vertical tubes, and for horizontal with $Fr_l > 0.04$

Table 2
Mean deviation and accuracy of three correlations for flow boiling heat transfer coefficient h

	Mean deviation (%)	Accuracy defined as fraction of data within ±30% error (%)
Modified Chen-type correlation in present study	13.6	93.6
Kandlikar [11]	19.7	80.7
Gungor and Winterton [9]	20.5	77.5

Mean deviation $= \frac{1}{n}\sum_1^n \frac{|h_{\mathrm{exp}} - h_{\mathrm{cal}}|}{h_{\mathrm{exp}}} \times 100\%$, where n is the number of data points.

$$x_{\text{dryout}} = \frac{s\left(1-\frac{2\delta_{\text{crit}}}{D}\right)^2\left(\frac{\rho_g}{\rho_l}\right)}{1-\left(1-\frac{2\delta_{\text{crit}}}{D}\right)^2\left[1-s\left(\frac{\rho_g}{\rho_l}\right)\right]}. \quad (12)$$

Fig. 3 shows δ_{crit} vs. Bo for three different diameter tubes ($D = 3.1$-, 1.12- and 0.51-mm-ID). These results show that δ_{crit} did not depend either on Bo or D and the average δ_{crit} was 15 μm (solid line in Fig. 3). Carey et al. [28] investigated two-phase heat transfer characteristics for refrigerant R-113 flow boiling with the large-scale offset fin and cross-ribbed geometries, and reported that $10 < \delta_{\text{crit}} < 37$ μm. The mean value of δ_{crit} obtained in this study is close to that reported by Carey et al. Fig. 4 compares the effect of D on x_{dryout} calculated from Eq. (12) using three different s (Eqs. (9)–(11)). The calculated x_{dryout} decreased with decreasing D, agreeing well with the tendency of experimental results by our previous study, Oh et al. [19] and Kattan et al. [29]. At $D \leqslant 2$ mm, the dryout quality x_{dryout} vs. tube diameter D curve calculated with the minimum momentum model (Eq. (9)) was closest to the experimental data. Kattan's experimental data [29] for a tube with large D (10.92-mm-ID) are smaller than the calculation results, suggesting that for a large D tube, dryout initially occurs on the top of the tube due to the effect of gravity. Figs. 5a–c compare the experimental x_{dryout} (x_{exp}) for our previ-

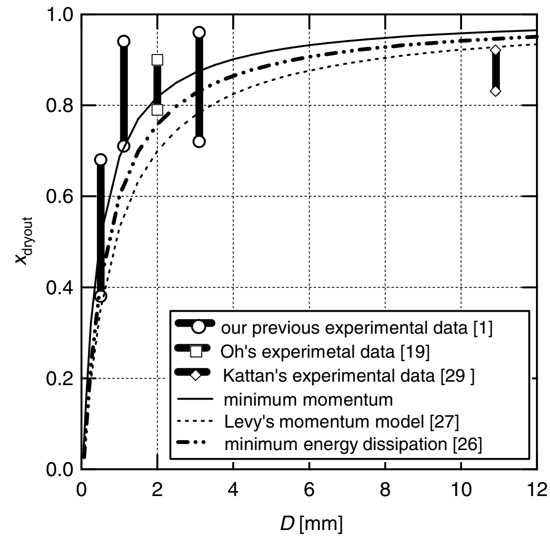

Fig. 4. Experimental dryout quality x_{dryout} vs. tube diameter D and calculated x_{dryout} vs. D based on the annular flow model shown in Fig. 2.

Table 3
Correlations for predicting dryout quality x_{dryout}

	Correlation for predicting x_{dryout}
Sun and Groll [15]	$x_{\text{dryout}} = x_{\text{crit}} - \frac{\Delta x_{\text{crit}}}{2}$ where $x_{\text{crit}} = 10.795\left(\frac{q}{1000}\right)^{-0.125} G^{-0.333}(1000D)^{-0.07} e^{0.01715p\times10^{-5}}$, for 0.49 MPa $\leqslant p \leqslant$ 2.94 MPa; $x_{\text{crit}} = 19.398\left(\frac{q}{1000}\right)^{-0.125} G^{-0.333}(1000D)^{-0.07} e^{-0.00255p\times10^{-5}}$, for 2.94 MPa $\leqslant p \leqslant$ 9.8 MPa; $x_{\text{crit}} = 32.302\left(\frac{q}{1000}\right)^{-0.125} G^{-0.333}(1000D)^{-0.07} e^{-0.00795p\times10^{-5}}$, for 9.8 MPa $\leqslant p \leqslant$ 19.6 MPa; $Fr = \frac{x_{\text{crit}} G/\sqrt{\rho_g}}{\sqrt{gD(\rho_l-\rho_g)\cos\theta}}$, $\theta = 0$ for horizontal flow; $\Delta x_{\text{crit}} = \frac{16}{(2+Fr)^2}$
Katto [30]	$x_{\text{dryout}} = 4\left(\frac{L}{D}\right)\left(\frac{q}{GH_{lg}}\right)$ where, L regime; $\frac{q}{GH_{lg}} = C\left(\frac{\sigma\rho_l}{G^2L}\right)^{0.043}\left(\frac{L}{D}\right)^{-1}$, $C = 0.25$ for $L/D < 50$, $C = 0.34$ for $L/D > 150$, $C = 0.25 + 0.0009\left[\left(\frac{L}{D}\right) - 50\right]$ for $50 \leqslant \frac{L}{D} \leqslant 150$

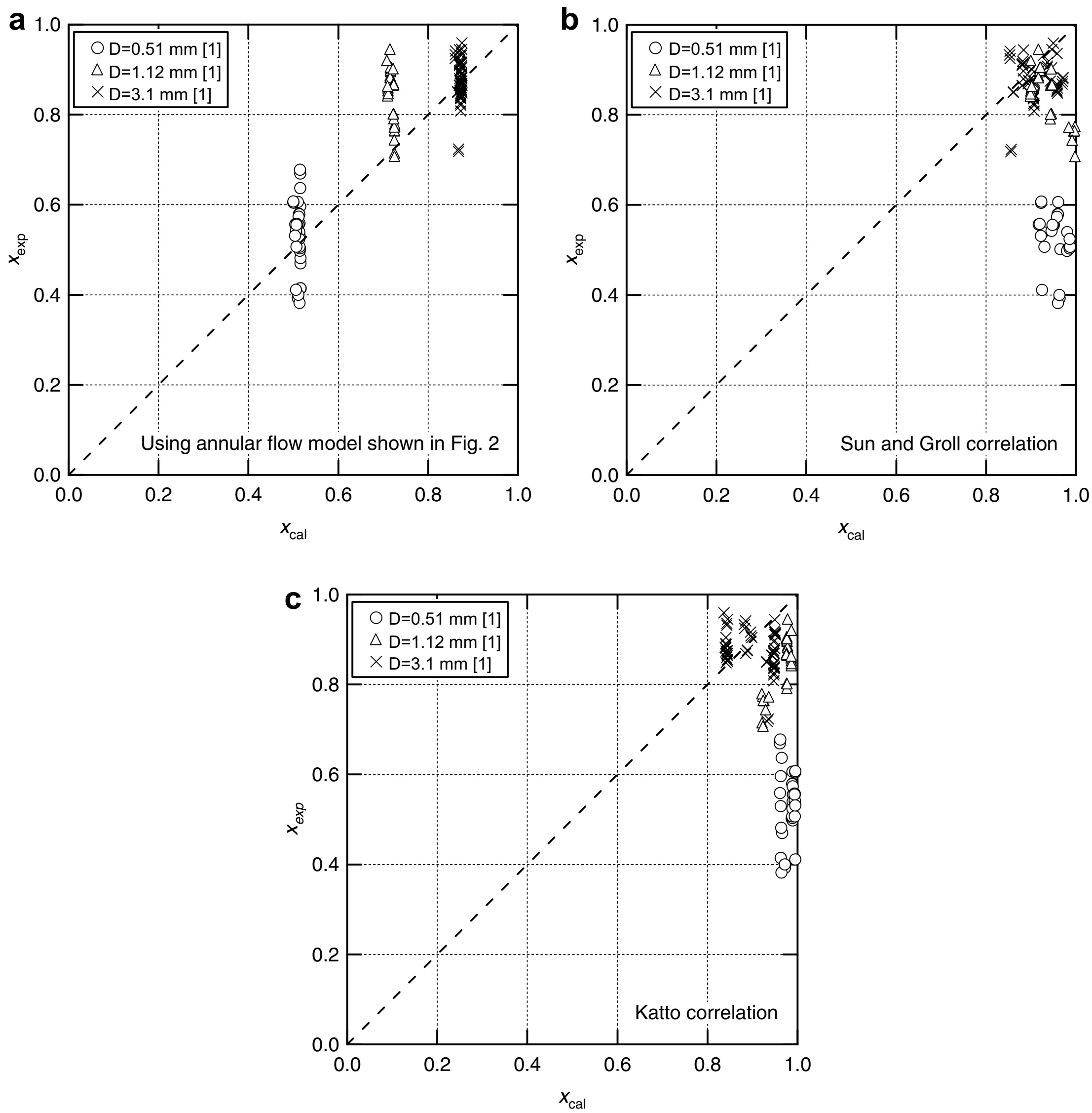

Fig. 5. Experimental dryout quality x_{exp} [1] and calculated x_{cal} based on (a) the annular flow model shown in Fig. 2, (b) Sun and Groll correlation [15], and (c) Katto correlation [30].

ous study and calculated x_{dryout} (x_{cal}) based on our annular flow model, Sun and Groll correlation [15], and Katto correlation [30], respectively, for three different D tubes. Table 3 summarizes the Sun and Groll correlation and Katto correlation. The present correlation based on the annular flow model agrees with the measured x_{dryout} for all three tubes; however, neither the Sun and Groll correlation nor Katto correlation can predict x_{dryout} for the smaller tubes (0.51- and 1.12-mm-ID). Both in the Sun and Groll correlation and the Katto correlation, dryout quality slightly increases with decreasing D. This tendency is opposite to that of the experimental results.

2.3. Post-dryout heat transfer

Fig. 6 shows typical results for the measured boiling heat transfer coefficient (h_{exp}) and the standard deviation (S.D.) of the measured temperature of the outer surface of the tubes as a function of x. The standard deviation was defined as $\mathrm{S.D.} = \sqrt{\sum_1^n \left(T_{\mathrm{W}} - \overline{T_{\mathrm{W}}}\right)^2/(n-1)}$, where T_{W}, $\overline{T_{\mathrm{W}}}$ and n are the measured temperature of the outer surface of the tubes, the mean value of T_{W}, and the number of measured data, respectively. After the onset of dryout, h_{exp} decreased and fluctuation in T_{W} increased with increasing x, suggesting that the dry-portion changes spatially and temporally on a tube wall. Based on measurements of R-141b flow boiling in single 1.39- to 3.69-mm-ID tubes, Kew and Cornwell [31] reported that dryout occurred locally and temporally in confined bubble flow and annular slug flow regimes. The flow patterns in small-diameter tubes in our previous study [1] are consistent with those by Kew and Cornwell. Thus, the occurrence of dry-portions causes decrease in h_{exp} and fluctuations in T_{W}.

Fig. 7 shows a simple flow model based on the annular flow in the post-dryout region. The heat transfer coefficient in the post-dryout region $h_{\mathrm{TP,post}}$ is given as

$$h_{\mathrm{TP,post}} = (1 - A_{\mathrm{D}})h_{\mathrm{TP,pre}} + A_{\mathrm{D}}h_{\mathrm{g}}, \tag{13}$$

where A_{D} is the ratio of the dry-portion around the entire perimeter of a tube, and $h_{\mathrm{TP,pre}}$ and h_{g} are the heat transfer coefficients for the liquid and gas fractions, respectively. The heat transfer coefficient h_{g} is given by the Dittus–Boelter equation:

$$h_{\mathrm{g}} = 0.023\frac{\lambda_{\mathrm{g}}}{D}Re_{\mathrm{g}}^{0.8}Pr_{\mathrm{g}}^{0.4}, \tag{14}$$

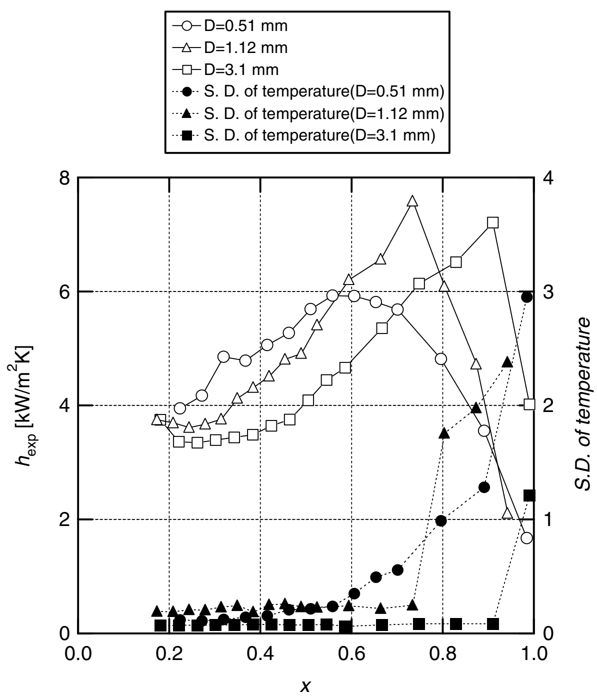

Fig. 6. Experimental boiling heat transfer coefficient h_{exp} and standard deviation of temperature (S.D.) [1] of the outer surface of a tube vs. vapor quality x for different inside tube diameter D, mass flux m, and heat flux q. For $D = 0.51$ mm, $m = 289$ kg/m^2 s and $q = 12.8$ kW/m^2. For $D = 1.12$ mm, $m = 298$ kg/m^2 s and $q = 13.2$ kW/m^2. For $D = 3.1$ mm, $m = 304$ kg/m^2 s and $q = 12.1$ kW/m^2.

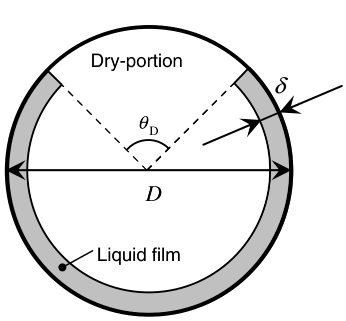

Fig. 7. Simple flow model based on the annular flow model shown in Fig. 2. Ratio of dry-portion and liquid film after the onset of dryout. D is the inner diameter of a tube, δ is the liquid film thickness. The ratio of the dry-portion around the entire perimeter of a tube is defined as $A_{\mathrm{D}} = \theta_{\mathrm{D}}/2\pi$.

where Re_{g} is the Reynolds number of the gas and is $Re_{\mathrm{g}} = \frac{GDx}{\mu_{\mathrm{g}}}$. From Eq. (13), A_{D} is given by

$$A_{\mathrm{D}} = \frac{h_{\mathrm{exp}} - h_{\mathrm{TP,pre}}}{h_{\mathrm{g}} - h_{\mathrm{TP,pre}}}. \tag{15}$$

Fig. 8 shows the relation between A_{D} and x normalized by x_{dryout} given by Eq. (12) as $x_{\mathrm{nor}} = \frac{x - x_{\mathrm{dryout}}}{1 - x_{\mathrm{dryout}}}$. The wide scatter in the data is due to significant fluctuation in the wall temperature after the onset of dryout. When the liquid flow is laminar ($Re_{\mathrm{l}} < 1000$) in the 0.51- and 1.12-mm-ID tubes, A_{D} can be fitted with a curve represented as $A_{\mathrm{D}} = -x_{\mathrm{nor}}^3 + x_{\mathrm{nor}}^2 + x_{\mathrm{nor}} - 0.03$ over a wide range of x_{nor}, whereas when the liquid flow is turbulent ($Re_{\mathrm{l}} > 1000$) in the 1.12-mm-ID tube, the fitted curve is $A_{\mathrm{D}} = 4(x_{\mathrm{nor}} - 0.5)^2$ in the range of $0.5 \leqslant x_{\mathrm{nor}} \leqslant 1$. Thus, these results suggest that the liquid film on a tube wall is maintained until higher x without partial dryout in liquid turbulent flow than in laminar flow. After onset of dryout, β is given as a function of A_{D} and δ as

$$\beta = 1 - \left[1 - \left(1 - \frac{2\delta}{D}\right)^2\right](1 - A_{\mathrm{D}}). \tag{16}$$

By eliminating β from Eqs. (8), (9) and (16), δ is given as function of A_{D} and x as

$$\frac{2\delta}{D} = 1 - \left[1 - \frac{1}{1 - A_{\mathrm{D}}}\left[1 - \frac{1}{1 + \frac{1-x}{x}\left(\frac{\rho_{\mathrm{g}}}{\rho_{\mathrm{l}}}\right)^{0.5}}\right]\right]^{0.5}. \tag{17}$$

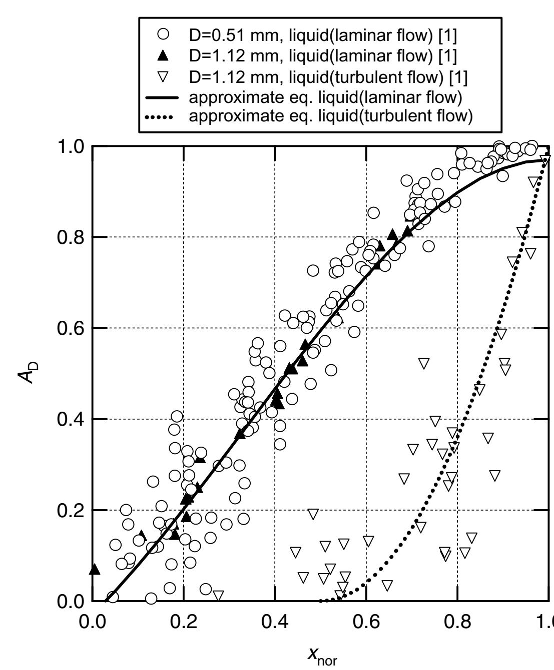

Fig. 8. Ratio of dry-portion A_{D} vs. normalized quality x_{nor}. A_{D} represents the ratio of dry-portion around the tube perimeter after the onset of dryout, and is given by Eq. (15). Normalized quality x_{nor} is defined as $\frac{x - x_{\mathrm{dryout}}}{1 - x_{\mathrm{dryout}}}$, and x_{dryout} is given by Eq. (12). Fitted curves are $A_{\mathrm{D}} = -x_{\mathrm{nor}}^3 + x_{\mathrm{nor}}^2 + x_{\mathrm{nor}} - 0.03$ for liquid laminar flow ($Re_{\mathrm{l}} < 1000$) and $A_{\mathrm{D}} = 4(x_{\mathrm{nor}} - 0.5)^2$ for liquid turbulent flow ($Re_{\mathrm{l}} > 1000$).

Fig. 9 shows the non-dimensional δ/δ_{crit} as a function of x_{nor} calculated with Eq. (17) by using experimental data (symbols) and the fitted curves of A_D. For turbulent liquid flow in the 1.12-mm-ID tube, δ/δ_{crit} decreased with increasing x_{nor}, whereas for liquid laminar flow, δ/δ_{crit} remained relatively constant at $x_{nor} < 0.6$. The mean and deviation of δ/δ_{crit} increased with increasing x_{nor} at $x_{nor} > 0.6$. This experimental result suggests that in liquid laminar flow, the liquid film breaks into small "streaks" whose average thickness could be larger than δ_{crit} due to cohesion of liquid, and that these streaks flow downstream while evaporating. Fig. 10 compares the measured and calculated h

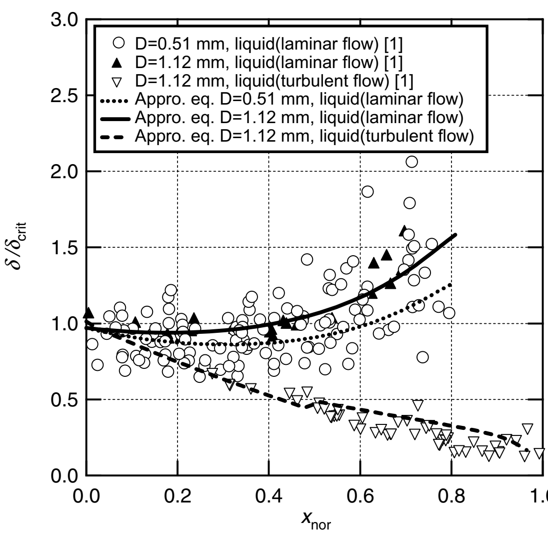

Fig. 9. Non-dimensional thickness of liquid film δ/δ_{crit} vs. normalized quality x_{nor} (for a critical liquid film thickness $\delta_{crit} = 15\ \mu m$). Curves were calculated using Eq. (17) with fitted curves $A_D = -x_{nor}^3 + x_{nor}^2 + x_{nor} - 0.03$ for liquid laminar flow ($Re_l < 1000$) and $A_D = 4(x_{nor}-0.5)^2$ for liquid turbulent flow ($Re_l > 1000$).

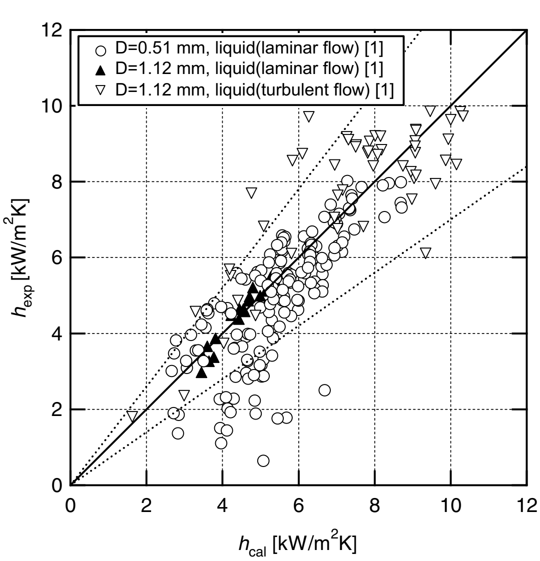

Fig. 10. Experimental heat transfer coefficient h_{exp} after onset of dryout [1] vs. calculated heat transfer coefficient h_{cal} based on Eq. (13).

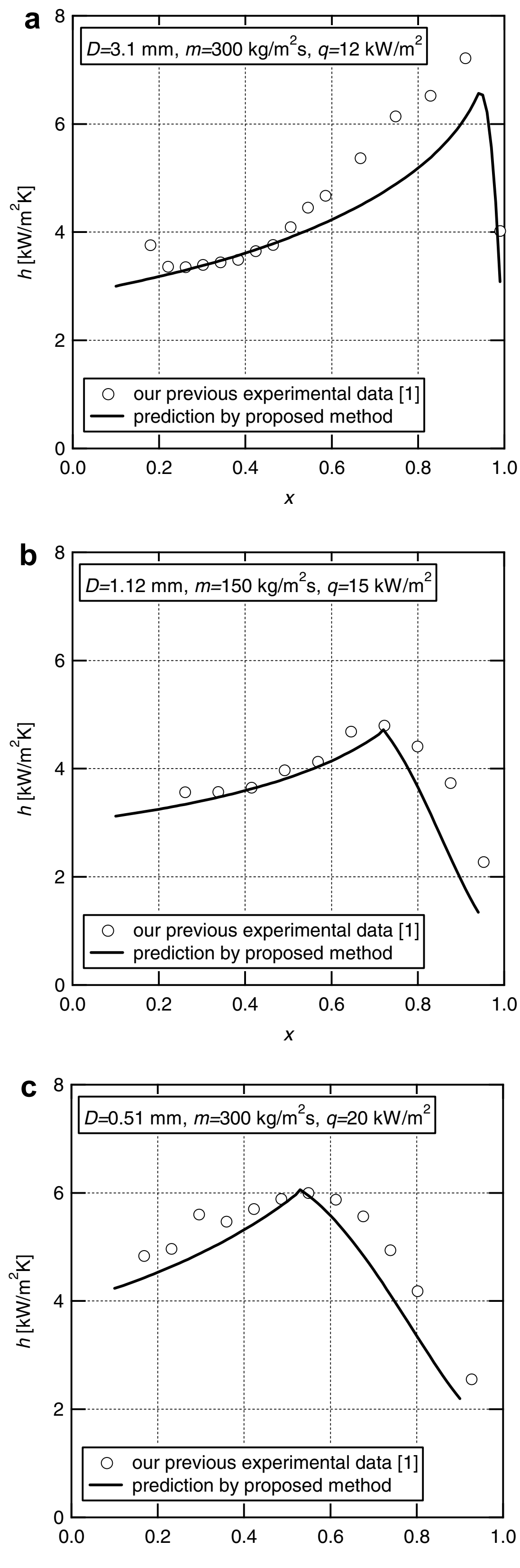

Fig. 11. Experimental heat transfer coefficient h_{exp} vs. calculated heat transfer coefficient h_{cal} for different inside tube diameter D, mass flux m, and heat flux q: (a) $D = 3.1$ mm, $m = 300\ kg/m^2\ s$ and $q = 12\ kW/m^2$; (b) $D = 1.12$ mm, $m = 150\ kg/m^2\ s$ and $q = 15\ kW/m^2$; and (c) $D = 0.51$ mm, $m = 300\ kg/m^2\ s$ and $q = 20\ kW/m^2$.

after the onset of dryout. When $h > 5\ \mathrm{kW/m^2\,K}$, h_{cal} given by Eq. (13) agrees well with h_{exp} in the range of ±30%. When $h < 5\ \mathrm{kW/m^2\,K}$, the data at $x > 0.9$ includes data where the measured temperature widely fluctuates, thus the h_{exp} deviates significantly from h_{cal}.

Figs. 11a–c show representative comparisons between predicted and measured h over a wide range of x for a 3.1-mm-ID tube (Fig. 11a), 1.12-mm-ID (Fig. 11b), and 0.51-mm-ID (Fig. 11c). The calculated $h_{TP,pre}$ and $h_{TP,post}$ vs. x relation and x_{dryout} agree well with the measured ones. The predicted heat transfer coefficients decrease sharply at dryout, because A_D increases rapidly with increasing x after the onset of dryout.

3. Conclusions

Correlations for the boiling heat transfer of R-134a in horizontal tubes including the effect of tube diameter were developed here for both the pre- and post-dryout regions. A simple annular flow model for the prediction of the onset of dryout was also developed. The results can be summarized as follows.

1. A modified Chen-type correlation for the flow boiling heat transfer was developed that included the effect of tube diameter. In this correlation, the effect of tube diameter on flow boiling heat transfer was characterized by the Weber number. The correlation agreed reasonably well with experimental data for a wide range of tube diameter from 0.51 to 10.92 mm ID.
2. A simple annular flow model was developed for prediction of dryout quality depending on the effect of tube diameter. The dryout quality predicted using this model agreed well with experimental data.
3. The heat transfer coefficient in the post-dryout region was predicted as the summation of two terms: the heat transfer coefficient by the Dittus–Boelter's correlation in the vapor phase and the pre-dryout heat transfer coefficient in the liquid phase. Both terms are a function of the dry-portion of the inner tube wall, and this dry-portion was estimated from experimental data. The calculated heat transfer coefficient agreed well with measured data within a range of ±30%.

References

[1] S. Saitoh, H. Daiguji, E. Hihara, Effect of tube diameter on the boiling heat transfer of R-134a in horizontal small tubes, Int. J. Heat Mass Transfer 48 (2005) 4973–4984.
[2] V.P. Carey, Liquid–Vapor Phase-Change Phenomena, Hemisphere, Washington D.C., 1992, pp. 483–564.
[3] V.E. Schrock, L.M. Grossman, Forced convection boiling in tubes, Nucl. Sci. Eng. 12 (1962) 474–481.
[4] Z. Liu, R.H.S. Winterton, A general correlation for saturated and subcooled flow boiling in tubes and annuli, based on a nucleate pool boiling equation, Int. J. Heat Mass Transfer 34 (1991) 2759–2766.
[5] D. Steiner, J. Taborek, Flow boiling heat transfer in vertical tubes correlated by an asymptotic model, Heat Transfer Eng. 13 (1992) 43–69.
[6] M.W. Wambsganss, D.M. France, J.A. Jendrzejczyk, T.N. Tran, Boiling heat transfer in a horizontal small-diameter tube, ASME J. Heat Transfer 115 (1993) 963–972.
[7] J.C. Chen, Correlation for boiling heat transfer to saturated fluids in convective flow, Ind. Eng. Chem. Proc. Des. Dev. 5 (1966) 322–329.
[8] K.E. Gungor, R.H.S. Winterton, A general correlation for flow boiling in tubes and annuli, Int. J. Heat Mass Transfer 29 (1986) 351–358.
[9] K.E. Gungor, R.H.S. Winterton, Simplified general correlation for saturated flow boiling and comparisons of correlations, Chem. Eng. Res. Des. 65 (1987) 148–156.
[10] M.M. Shah, A new correlation for heat transfer during boiling flow through pipes, ASHRAE Trans. 82 (1976) 66–86.
[11] S.G. Kandlikar, A general correlation for saturated two-phase flow boiling heat transfer inside horizontal and vertical tubes, ASME J. Heat Transfer 112 (1990) 219–228.
[12] J.B. Chaddock, H.K. Varma, An experimental investigation of dry-out with R-22 evaporating in a horizontal tube, ASHRAE Trans. 85 (1979) 105–121.
[13] Y. Katto, Critical heat flux, Int. J. Multiphase Flow 20 (1994) 53–90.
[14] Y. Katto, On the heat–flux/exit-quality type correlation of CHF of forced convection boiling in uniformly heated vertical tubes, Int. J. Heat Mass Transfer 24 (1981) 533–539.
[15] Z. Sun and E.A. Groll, CO_2 flow boiling heat transfer in horizontal tubes, Part 1: Flow regime and prediction of dryout, in: Proceedings of 5th IIR-Gustav Lorentzen Conference on Natural Working Fluids, 2002, pp. 131–140.
[16] K.A. Triplett, S.M. Ghiaasiaan, S.I. Abdel-Khalik, D.L. Sadowski, Gas–liquid two-phase flow in microchannels, Part I: Two-phase flow patterns, Int. J. Multiphase Flow 25 (1999) 377–394.
[17] S.M. Ghiaasiaan, S.I. Abdel-Khalik, Two-Phase Flow in Microchannels, Advances in Heat Transfer, vol. 34, Academic Press, 2001, pp. 145–254.
[18] K. Stephan, M. Abdelsalam, Heat-transfer correlations for natural convection boiling, Int. J. Heat Mass Transfer 23 (1980) 73–87.
[19] H.-K. Oh, M. Katsuta, K. Shibata, Heat transfer characteristics of R-134a in a capillary tube heat exchanger, in: Proceedings of 11th IHTC, vol. 6, 1998, pp. 131–136.
[20] L.S. Zhang, Dr. Thesis, University of Tokyo, 1996.
[21] S. Yoshida, H. Mori, K. Ohishi, Y. Takahashi, Flow boiling heat transfer to HFC134a in horizontal tubes, in: Thermal Engineering Symposium '94 No. 7, 1994, pp. 51–52.
[22] J.Y. Shin, M.S. Kim, S.T. Ro, Experimental study on forced convective boiling heat transfer of pure refrigerants and refrigerant mixtures in a horizontal tube, Int. J. Refrig. 20 (1997) 267–275.
[23] M.O. McLinden, S.A. Klein, E.W. Lemmon, A.P. Peskin, NIST Thermodynamic and Transport Properties of Refrigerants and Refrigerant Mixtures (REFPROP) Version 6.01, NIST, 1998.
[24] S.G. Kandlikar, P. Balasubramanian, An extension of the flow boiling correlation to transition, laminar, and deep laminar flows in minichannels and microchannels, Heat Transfer Eng. 25 (2004) 86–93.
[25] A.H. Govan, G.F. Hewitt, Prediction of dryout using phenomenological models, Int. J. Heat Technol. 10 (1992) 1–43.
[26] S.M. Zivi, Estimation of steady-state steam void-fraction by means of the principle of minimum entropy production, ASME J. Heat Transfer 86 (1964) 247–252.
[27] S. Levy, Steam slip-theoretical prediction from momentum model, ASME J. Heat Transfer 82 (1960) 113–124.
[28] V.P. Carey, P. Tervo, K. Shollenberger, Partial dryout in enhanced evaporator tubes and its impact on heat transfer performance, in: SAE Tech. Pap. Ser., 1992, pp. 1–9.

[29] N. Kattan, J.R. Thome, D. Favrat, Flow boiling in horizontal tubes: Part 2 – New heat transfer data for five refrigerants, ASME J. Heat Transfer 120 (1998) 148–155.
[30] Y. Katto, Prediction of critical heat flux for annular in tubes taking into account the critical liquid film thickness concept, Int. J. Heat Mass Transfer 27 (1984) 883–891.
[31] P.A. Kew, K. Cornwell, Correlations for the prediction of boiling heat transfer in small-diameter channels, Appl. Therm. Eng. 17 (1997) 705–715.